LECTURE 25

Sediment Oxygen Demand

LECTURE OVERVIEW: I review typical SOD values observed in natural waters and then outline mechanistic approaches for modeling the phenomenon. I first derive a simple model that is consistent with the classic Streeter-Phelps paradigm. Then I describe a more realistic framework that accounts for phenomena such as gas formation and hence provides a superior approach for simulating SOD in natural waters.

Sediment oxygen demand or SOD is due to the oxidation of organic matter in bottom sediments. These benthic deposits or "sludge beds" derive from several sources. Wastewater particulates. as well as other allochthonous particulates (leaf litter and eroded organic-rich soils), can result in sediments with high organic content. In addition. in highly productive environments such as eutrophic lakes. estuaries, and rivers. photosynthetically produced plant matter can settle and accumulate on the bottom. Regardless of the source. oxidation of the accumulated organic matter will result in a sediment oxygen demand.

As mentioned previously in Lec. 22, the first attempts to model SOD used a zero-order or constant source term. Such a characterization was deemed adequate when water-quality models were primarily used to assess the impact of treating raw sewage. However. as treatment becomes more refined and concern for nonpoint sources grows. such characterizations become increasingly inadequate. This is due to the fact that there is no satisfactory way to decide how the SOD changes following treatment.

The two most common approaches were to (1) leave the SOD unchanged or (2) assume linearity and lower SOD in direct proportion to the load reduction. Such arbitrary methods were usually justified under the assumption that a truly mechanistic understanding of the process was not necessary when making crude assessments of the etfects of primary and secondary treatment. Although this assumption is probably

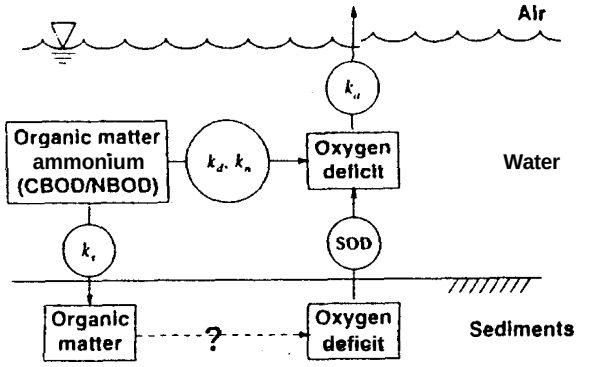

FIGURE 25.1
The "missing link" between settling losses and SOD in classical Streeter-Phelps theory.

questionable in itself. it becomes even more tenuous as models are used to evaluate advanced waste treatment.

Such shortcomings arise because the zero-order approach treats SOD as a model input rather than as a calculated variable. This problem is illustrated in Fig. 25.1. Recall that in our earlier discussion of the Streeter-Phelps model. we included a parameter, k_s, to simulate that particulate sewage can be removed by settling. Later. we expanded the model to include the zero-order SOD to simulate the oxygen demand due to the decomposition of the settled sewage in the bottom sediments. As illustrated in Fig. 25.1, there is a missing piece that was left out of the process. That is. the use of the zero-order SOD neglects the mechanism whereby the sediment organic matter is converted into oxygen demand.

The present lecture is designed to show how this missing link can be modeled. To do this. I will first review data in order to delineate the levels that occur in natural waters and the major factors that influence SOD. Then I will construct a simple "Streeter-Phelps" SOD model which, although it is unrealistic, provides a context for our subsequent discussions. Finally 1 describe a more recently developed framework for calculating SOD in a mechanistic fashion.

25.1 OBSERVATIONS

SOD is typically measured in three ways: two approaches based on modeling observed oxygen levels and one based on direct measurement. In the first model-based approach. a DO model is developed for the water body and all rates except the SOD are determined. The SOD can then be estimated by adjusting the SOD rate until the model predictions match the observed DO levels. Although this calibration method was widespread in the early years of modeling. it is flawed because it assumes that all other model parameters (reaeration, deoxygenation rates, etc.) are known with confidence. Because such is rarely the case, values obtained with this method are no better than order-of-magnitude estimates.

The second model-based approach is expressly designed for stratified lakes. For such systems the deeper waters (or hypolimnion) can be idealized as a closed system, and an areal hypolimnetic oxygen demand can be determined as

$$\text{AHOD} = \frac{o_2 - o_1}{t_2 - t_1} H_h \tag{25.1}$$

where AHOD = areal hypolimnetic oxygen demand (gO m^{-2} d^{-1})
o_1 and o_2 = hypolimnetic oxygen levels (mg L^{-1}) measured at two times, t_1 and t_2 (d), during the stratified period
H_h = mean thickness of the hypolimnion (m)

If it is assumed that the primary cause of oxygen depletion in this layer is decomposition of organic matter in or at the surface of the bottom sediments, the oxygen depletion over the summer-stratified period provides an estimate of the SOD. That is, we assume that $S'_B \cong$ AHOD.

This approach has a number of deficiencies that relate to its underlying assumptions. First, it does not distinguish between decomposition in the water column and in the sediments. Whereas the former is not usually as important as the latter, in deeper systems the assumption might be violated. Second, although strong thermal gradients diminish mass transfer between the surface and bottom water layers, some transport does occur. It should be noted that corrections can be made to account for thermocline transport (Chapra and Reckhow 1983). However, since such corrections have rarely been made, most literature AHOD values usually represent underestimates of the actual depletion.

The final estimation method involves direct measurement. This is done by enclosing the sediments and some overlying water in a chamber and measuring the dissolved oxygen concentration in the water as a function of time. This approach is used in both the laboratory and the field. As with all microcosm measurements (e.g., the BOD or light-bottle/dark-bottle tests), this test has the drawback that enclosing the water in a chamber makes the system different from the natural environment.

Typical values of SOD are listed in Table 25.1. In general, values from about 1 to 10 g m^{-2} d^{-1} are considered indicative of enriched sediments. Also notice that the organism *Sphaerolitus* is included in the table to indicate that benthic organisms other than bacteria can process organic matter from the overlying water and exert an SOD (see Box 25.1).

TABLE 25.1
Sediment oxygen demand values (from Thomann 1972 and Rast and Lee 1978)

Bottom type and location	$S'_{B,20}$ (g m^{-2} d^{-1})	
	Average value	Range
Sphaerolitus (10 g-dry wt m^{-2})	7	—
Municipal sewage sludge:		
Outfall vicinity	4	2–10
Downstream of outfall, "aged"	1.5	1–2
Estuarine mud	1.5	1–2
Sandy bottom	0.5	0.2–1
Mineral soils	0.07	0.05–1
Areal hypolimnetic oxygen demand (AHOD)—lakes		0.06–2

The effect of temperature on SOD can be represented by

$$S'_B = S'_{B,20}\theta^{T-20} \tag{25.2}$$

where $S'_{B,20}$ = areal SOD rate at 20°C and θ = temperature coefficient. Zison et al. (1978) have reported a range of 1.04 to 1.13 for θ. A value of 1.065 is commonly employed. In addition the SOD for temperatures below 10°C typically declines faster than indicated by Eq. 25.2. In the range from 0 to 5°C, it approaches zero.

BOX 25.1. ZOD or "Zebra Mussel Oxygen Demand"

You may have noticed that along with typical environmental settings, Table 25.1 contains the organism *Sphaerolitus*. These organisms are attached, filamentous higher bacteria that are commonly and erroneously called "sewage fungus." They typically grow in channels dominated by raw sewage, and as noted, their respiration results in a high oxygen demand.

Other bottom organisms can have a similar effect. Among the most notorious are the freshwater mollusks commonly called zebra mussels (*Dreissena polymorpha*). Originally native to the Caspian Sea/Black Sea region, they were probably introduced into the Great Lakes in the late 1980s when a ship from Europe released its ballast water into Lake St. Clair (Ludyanskiy et al. 1993, Mackie 1991). This freshwater mollusk attaches to lake and river bottoms, channels, and pipe walls. To date, the biggest problem connected with the organism is clogging at drinking and cooling water intake pipes. However, recent evidence suggests that they can also have a significant effect on water quality.

One such case occurs in the Seneca River, N.Y., a tributary of Lake Ontario. In 1993 the Upstate Freshwater Institute (U.F.I.) in Syracuse, N.Y., conducted a study of a 16-km section of the river that was infested with the mussels. Steve Effler, Clifford Siegfried, and Ray Canale measured (Effler and Siegfried 1994) and modeled (Canale and Effler 1995) the section, and their results document the impact of the organism.

They measured an average mussel density over the stretch of 6000 individuals m^{-2}. They then independently measured an organism respiration rate of 0.9 mgO $individual^{-1}$ d^{-1}. The product of these numbers yielded an oxygen demand, or as dubbed by Prof. Canale, a "ZOD," of 5.4 gO m^{-2} d^{-1}. Together with other measured parameters for the section, they used a simple oxygen model of the form of Eq. 22.12 to determine that oxygen levels should drop to about 3.9 mg L^{-1} at the end of the stretch. As depicted in Fig. B25.1, this prediction conforms nicely to measurements. Beyond that the model predicts that 80% of the oxygen demand is due to zebra mussel respiration.

The zebra mussels also have a dramatic effect on the nutrients in the system. The mussels in the reach filter water at a rate of 60 m^3 s^{-1}. This organism "flow rate" is 2 times the flow rate in the river! As they filter, they take in and consume floating phytoplankton. As a consequence, chlorophyll *a* levels in the stretch drop from 45 to 5 μg L^{-1}. At the same time, the mussels excrete and egest soluble phosphorus and ammonium, leading to increases of 48 μgP L^{-1} and 0.4 mgN L^{-1}, respectively. Although the phosphorus increase is consistent with model results, the ammonium observations are less than predicted. However, this discrepancy can be attributed to nitrification.

In summary, aside from its other nuisance impacts, the zebra mussel can also directly impact water chemistry and quality through their metabolism and processing of

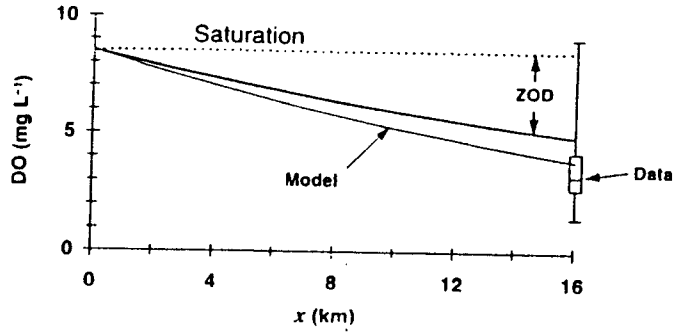

FIGURE B25.1

organic matter. The more general theme of such biological impacts will be elaborated on in great detail when we describe eutrophication in the next part of this book.

Aside from temperature, the two other factors that affect SOD are the organic content of the sediments and the oxygen concentration of the overlying waters. Baity (1938) and Fair et al. (1941) provided the first evidence of how the organic content of the sediments affected SOD. Their work suggests a square-root relationship between the SOD and the sediment volatile solids. A similar effect is provided by Fig. 25.2*a*, which correlates SOD with sediment COD.

AHOD also seems to be related to lake total phosphorus concentration by a square-root dependency (Fig. 25.2*b*). Because lakes with high phosphorus tend to have high productivity, such systems would be expected to have elevated sediment organic-carbon content. Thus Fig. 25.2*b* seems to imply the same square-root relationship between SOD and sediment carbon. In summary all the data displayed in Fig. 25.2 lead to the general conclusion that there is less SOD per organic carbon as the sediments become more enriched.

Oxygen is the other factor that affects SOD. Clearly if water oxygen concentration goes to zero the SOD will cease. Conversely above a certain level, it is usually assumed that the SOD is independent of the oxygen concentration in the overlying

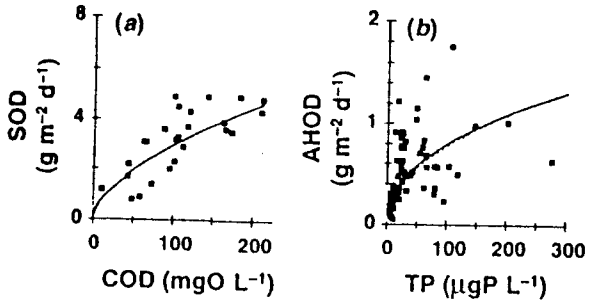

FIGURE 25.2
Two sets of observations that indicate a square-root relationship between SOD and organic content of sediments. (*a*) SOD versus surface sediment COD (Gardiner et al. 1984); (*b*) AHOD versus total phosphorus concentration (Rast and Lee 1978, Chapra and Canale 1991).

waters. Baity (1938) concluded that this was the case for oxygen levels greater than 2 mg L^{-1}. Several investigators have tried to represent the dependence by a saturating relationship,

$$S'_B(o) = \frac{o}{k_{so} + o} S'_B \tag{25.3}$$

where $S'_B(o)$ = oxygen-dependent SOD
o = oxygen concentration of the overlying water (mg L^{-1})
k_{so} = half-saturation value for the dependence (mg L^{-1})

Lam et al. (1984) have suggested a value for k_{so} of 1.4 mg L^{-1}. Thomann and Mueller (1987) fit the data of Fillos and Molof (1972) with a value of k_{so} = 0.7 mg L^{-1}. This latter result corresponds to independence at oxygen concentrations greater than about 3 mg L^{-1}.

25.2 A "NAIVE" STREETER-PHELPS SOD MODEL

Initial efforts to develop a mechanistic representation of SOD took the logical step of simulating the sediment compartment in a similar fashion to the water column. The segmentation scheme for such a model is depicted in Fig. 25.3. Notice that the subscripts w and 2 will be used for water and sediments, respectively. In addition the water concentrations will not be simulated as state variables. Rather they will serve as boundary conditions for the sediments. Finally we will assume that the surface area of the water is equal to the surface area of the sediments and that the temperatures of the two segments are identical.

We can now develop sediment CBOD and NBOD mass balances using first-order kinetics. For CBOD the equation would be

$$V_2 \frac{dL_2}{dt} = k_s V_w L_w - k_{d2} V_2 L_2 \tag{25.4}$$

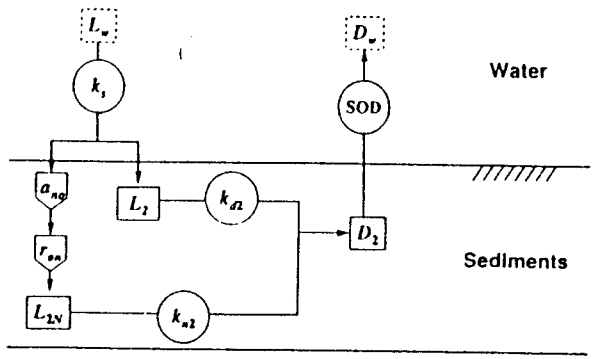

FIGURE 25.3
A "Streeter-Phelps" model for SOD. Note that the water concentrations of BOD and deficit are considered as boundary conditions, rather than state variables.

where k_{d2} = decomposition rate in the sediments (d^{-1}). At steady-state this balance can be solved for

$$L_2 = \frac{k_s H_w}{k_{d2} H_2} L_w \tag{25.5}$$

where H = layer thickness (m).

A similar balance for NBOD can be written as

$$V_2 \frac{dL_{2n}}{dt} = a_{no} r_{on} k_s V_w L_w - k_{n2} V_2 L_2 \tag{25.6}$$

where a_{no} = stoichiometric yield of nitrogen from the decomposition of settling BOD

r_{on} = oxygen demand to nitrogen ratio due to nitrification = 4.57 gBOD gN^{-1}

k_{n2} = nitrification rate in the sediments (d^{-1})

Note that, according to the stoichiometric relationships from Eq. 23.21, the nitrogen yield can be calculated as

$$a_{no} = \frac{16(14)}{107(32)} = 0.0654 \text{ gN gBOD}^{-1} \tag{25.7}$$

At steady-state, Eq. 25.6 can be solved for

$$L_{2n} = 0.3 \frac{k_s H_w}{k_{n2} H_2} L_w \tag{25.8}$$

where we have substituted and combined the values for a_{no} and r_{on}. Thus we see that according to our simple model, the settling particulate CBOD carries an additional 30% of oxygen demand due to nitrification.

Finally the oxygen deficit balance can be written as

$$V_2 \frac{dD_2}{dt} = k_{d2} V_2 L_2 + k_{n2} V_2 L_{2n} - S'_B A_s \tag{25.9}$$

where A_s = area of the sediment water interface (m^2). At steady-state this balance can be solved for

$$S'_B = 1.3 k_s H_w L_w \tag{25.10}$$

It can further be simplified by realizing that

$$J_{C\cdot} = k_s H_w L_w = v_s L_{pw} \tag{25.11}$$

where $J_{C\cdot}$ = downward flux of organic carbon expressed as oxygen equivalents ($gO\ m^{-2}\ d^{-1}$)

v_s = settling velocity of particulate organics ($m\ d^{-1}$)

L_{pw} = particulate BOD concentration in the water ($mg\ L^{-1}$)

Substituting this relationship into Eq. 25.10 gives

$$S'_B = 1.3 J_{C\cdot} \tag{25.12}$$

Consequently the model yields the rather simple result that the steady-state SOD should be equal to about 130% of the downward flux of ultimate BOD. Table 25.2

TABLE 25.2
SOD in $g\ m^{-2}\ d^{-1}$ calculated with the "naive" Streeter-Phelps SOD model

Particulate CBOD ($mg\ L^{-1}$)	Settling velocity ($m\ d^{-1}$)		
	0.1	0.2	0.5
0.5	0.065	0.13	0.325
1	0.13	0.26	0.65
5	0.65	1.3	3.25
10	1.3	2.6	6.5
50	6.5	13	32.5
100	13	26	65

shows a matrix that applies this result with a range of organic settling velocities and particulate BODs that are typically encountered in natural waters. Thus our simple framework would lead us to conclude that SODs in natural waters should range between about 0.05 to 65 $g\ m^{-2}\ d^{-1}$. The upper end of this range is well beyond the typical values in Table 25.1. This overprediction occurs because Eq. 25.12 specifies a linear relationship between SOD and the downward flux of organics. This contradicts the square-root relationships depicted in Fig. 25.2. Thus we can conclude that our "naive" Streeter-Phelps SOD model is not capable of capturing the diminished oxygen demand for highly productive systems. At best it provides an upper bound on the process. Now we turn to a more sophisticated framework that is capable of simulating the square-root dependency.

25.3 AEROBIC AND ANAEROBIC SEDIMENT DIAGENESIS

In a landmark paper, Di Toro et al. (1990) developed a model of the SOD process that mechanistically arrives at the same square-root relationship exhibited by Fig. 25.2. Before plunging into its mathematics, we would first like to provide a more realistic description of how organic carbon decomposition (or diagenesis) leads to SOD.

As depicted in Fig. 25.4 the sediments are divided into an aerobic (oxidizing) and an anaerobic (reducing) zone. Within these zones both organic carbon and nitrogen undergo transformations that ultimately create SOD. We will describe them separately.

Carbon. Particulate organic matter (POM) is delivered to the sediments by settling. Within the anaerobic sediments, the organic carbon decomposes to yield dissolved methane,

$$CH_2O \rightarrow \tfrac{1}{2}CO_2 + \tfrac{1}{2}CH_4 \tag{25.13}$$

where CH_2O is a simplified representation of organic matter. The methane diffuses upward to the aerobic zone where it is oxidized,

$$\tfrac{1}{2}CH_4 + O_2 \rightarrow \tfrac{1}{2}CO_2 + H_2O \tag{25.14}$$

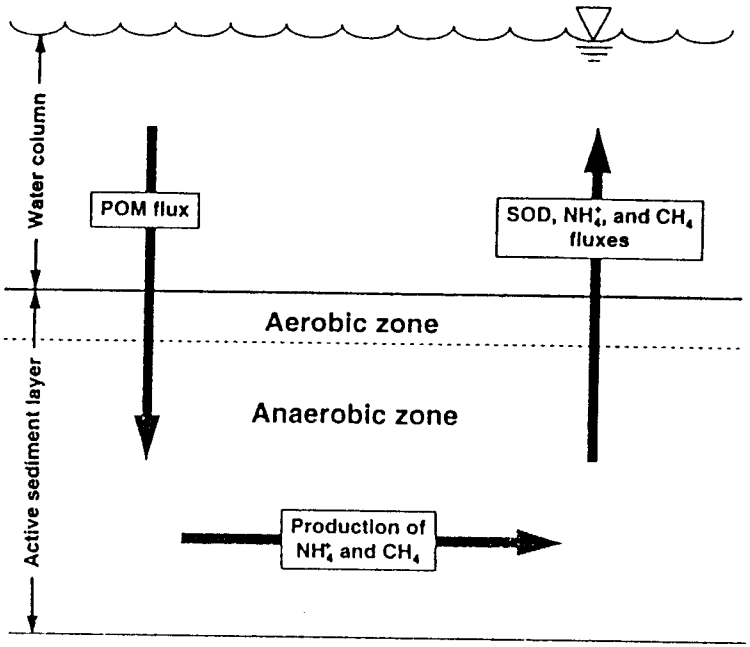

FIGURE 25.4
An overview of the mechanistic SOD framework (redrawn from Di Toro et al. 1990).

In the process an SOD is generated. Any residual methane that is not oxidized in the aerobic layer is diffused back into the water where additional oxidation can take place.

A problem with modeling this scheme is that we are dealing with several chemical species: CH_2O, CH_4, and O_2. Thus according to Eq. 25.13, 1 gC of organic matter would yield 0.5 gC of methane in the anaerobic sediments. Then, according to Eq. 25.14, the 0.5 gC of methane would consume 2.67 gO in the aerobic zone.

These conversions can be avoided by expressing all the species as ***oxygen equivalents***, that is, as the oxygen required for complete oxidation. Di Toro uses the nomenclature O* to distinguish oxygen equivalents from the actual oxygen concentration O_2. If this is done, 1 gO* of organic matter yields 1 gO* of methane that consumes 1 gO* of oxygen. Thus the need for stoichiometric conversions is unnecessary. It should be noted that the idea of oxygen equivalents should not be new to you. In fact we have already used them in the previous section when we used CBOD and NBOD to represent the oxygen equivalents of organic carbon and nitrogen.

Nitrogen. The two-zone scheme depicted in Fig. 25.4 also affects nitrogen. In the anaerobic zone, ammonium is generated via ammonification of organic N. Thus a gradient is created that feeds ammonium to the aerobic layer. In the aerobic zone, nitrification of the ammonium serves as an oxygen-demanding reaction that exerts

an NSOD. Ammonium that is not converted to nitrate diffuses back into the water by diffusion.

The oxidation of ammonium in the aerobic layer can be represented by

$$NH_3 + 2O_2 \rightarrow HNO_3 + H_2O \tag{25.15}$$

This reaction consumes 4.57 gO gN^{-1}, which together with the nitrogen yield from organic matter decomposition (0.0654 gN gO^{-1}) leads to the nitrogenous oxygen demand calculated previously in Eq. 25.8.

Now, in contrast to the simple model described in the previous section, nitrification is not the last step in the process. In fact much of the nitrate is denitrified to form nitrogen gas. If it is assumed that the carbon source for denitrification is methane, this reaction can be represented as

$$\tfrac{5}{8}CH_4 + HNO_3 \rightarrow \tfrac{5}{8}CO_2 + \tfrac{1}{2}N_2 + \tfrac{7}{4}H_2O \tag{25.16}$$

The entire process can be compressed into a single reaction by combining Eqs. 25.14 to 25.16 to give

$$NH_3 + \tfrac{3}{4}O_2 \rightarrow \tfrac{1}{2}N_2 + \tfrac{6}{4}H_2O \tag{25.17}$$

Thus the oxidation of the nitrogenous matter yields

$$r'_{on} = \frac{0.75(32)}{14} = 1.714 \text{ gO } gN^{-1} \tag{25.18}$$

where r'_{on} = oxygen demand for nitrification, corrected for denitrification.

This is an extremely important result since it indicates that the oxygen consumption would be much lower than the 4.57 gO gN^{-1} usually expected from the nitrification reaction. This reduction occurs because methane is consumed in the denitrification process. Consequently Eq. 25.12 should be adjusted to

$$S'_B = 1.11J_C. \tag{25.19}$$

Thus, rather than the 30% additional SOD due to nitrification (Eq. 25.12), the inclusion of denitrification lowers the increase to about 11%.

In summary the foregoing description does not lead to serious modifications to the simple Streeter-Phelps approaches described in the previous section. However, it does suggest that denitrification mitigates the NSOD effect. Next we see that modeling the vertical distribution of reactants in the sediments along with gas formation will have a much more significant impact on our calculations.

25.4 SOD MODELING (ANALYTICAL)

Di Toro and his colleagues used the framework described in the previous section to explain the square-root relationship of SOD to sediment organic carbon content. Their theory is depicted in Fig. 25.5. In essence when the organic carbon content of the sediment gets high, the amount of methane produced in the anaerobic sediments can exceed its solubility and bubbles form. These bubbles advect upward due to their buoyancy and consequently represent a loss of organic carbon that does not

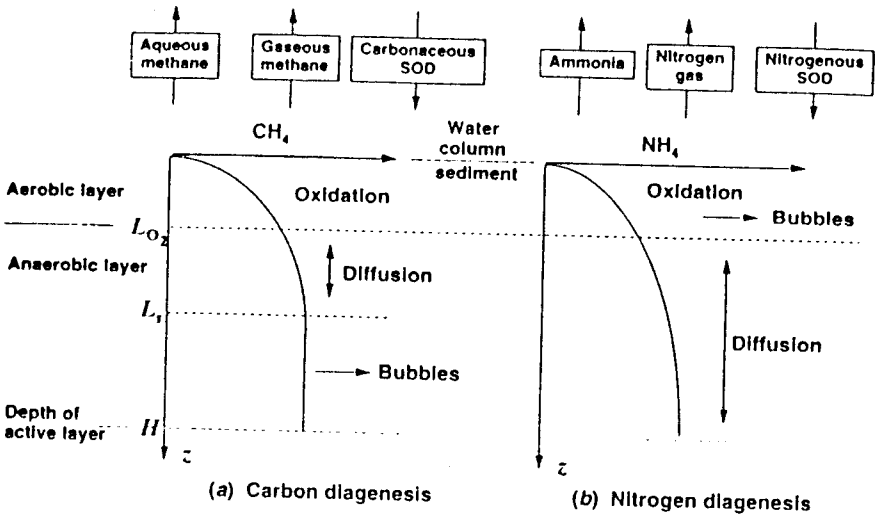

FIGURE 25.5
A schematic diagram of Di Toro's SOD model (redrawn from Di Toro et al. 1990).

exert a sediment oxygen demand. This loss is one component of the observed square-root relationship between SOD and sediment organic carbon content.

The following sections are intended to describe Di Toro's approach. Because the framework is somewhat complicated, I describe it in several parts. It is hoped that this will help you to understand it more thoroughly and, in so doing, appreciate its elegance.

25.4.1 A Simple Methane Balance

Rather than presenting the complete framework, we can develop a simplified version to gain insight into Di Toro's approach. To do this we initially concentrate on carbon. Then in a later section we broaden the framework to include nitrogen.

The active sediments can be idealized as a one-dimensional vertical system with a thickness H (Fig. 25.6). A mass balance for dissolved methane in the sediment

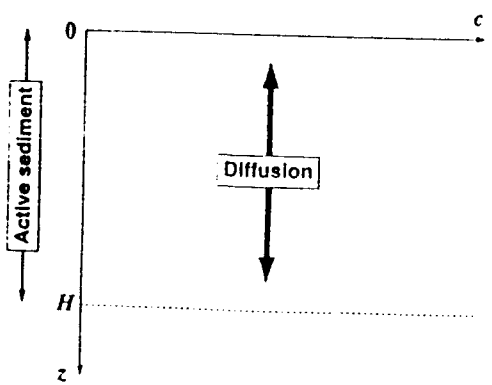

FIGURE 25.6
One-dimensional scheme for characterizing the vertical distribution of constituents in an active sediment layer.

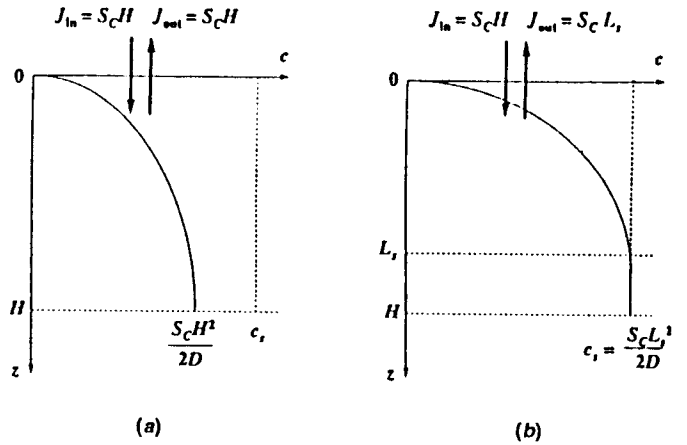

FIGURE 25.7
Vertical profile when methane in the pore waters (*a*) does not exceed and (*b*) does exceed saturation.

interstitial waters can be written as

$$0 = D\frac{d^2c}{dz^2} + S_C \tag{25.20}$$

where D = diffusion coefficient of methane in the sediment interstitial waters ($m^2\,d^{-1}$)
c = concentration of methane as measured in oxygen equivalents ($mgO\,L^{-1}$)
z = depth into the sediments (m)
S_C = a constant source of methane ($mgO\,L^{-1}\,d^{-1}$)

We can integrate this equation for two cases. In the first case we assume that the methane never exceeds saturation. Thus all methane is in dissolved form and no bubbles form. For this case the following boundary conditions can be assumed:

$$c(0) = 0 \tag{25.21}$$

$$\left.\frac{dc}{dz}\right|_{z=H} = 0 \tag{25.22}$$

The first condition specifies that the methane concentration of the overlying water is zero. The second stipulates that transport across the bottom of the active layer is zero.

Using these conditions, we can solve Eq. 25.20 for

$$c = \frac{S_C H z}{D} - \frac{S_C z^2}{2D} \tag{25.23}$$

As displayed in Fig. 25.7*a*, the solution is a parabola that is zero at the surface and increases to a maximum concentration at the bottom of the active sediments,

$$c(H) = \frac{S_C H^2}{2D} \tag{25.24}$$

Differentiation of Eq. 25.23 and substitution into Fick's first law shows that the flux of oxygen equivalents back to the water column is

$$J_{out} = D\frac{dc}{dz} = S_C H \tag{25.25}$$

As would be expected, the flux out corresponds to all the methane production in the active sediment layer. Since all the organic carbon in the sediment is assumed to be due to settling of particulates from the water column, this means that the flux out is equal to the flux in. Consequently if the methane never exceeds saturation, the linear model described in the previous section would be valid.

Next we look at a second case where the organic carbon levels are high enough that methane saturation is exceeded and, hence, bubbles form. For this case, along with the surface condition (Eq. 25.21), the following bottom boundary conditions hold:

$$c(L_s) = c_s \tag{25.26}$$

$$\left.\frac{dc}{dz}\right|_{z=L_s} = 0 \tag{25.27}$$

The first condition specifies that there is a depth L_s at which the methane concentration reaches saturation, c_s. The second condition stipulates that net transport across this depth is zero.

Employing these conditions, we can solve Eq. 25.20 for

$$c = c_s - \frac{S_C}{2D}(L_s - z)^2 \qquad z \le L_s \tag{25.28a}$$

$$c = c_s \qquad z > L_s \tag{25.28b}$$

As displayed in Fig. 25.7*b*, the solution is again parabolic. However, now it reaches saturation at a level L_s that is above the bottom of the active layer. This depth can be determined by substituting $c = 0$ and $z = 0$ into Eq. 25.28*a*, which can be solved for

$$L_s = \sqrt{\frac{2Dc_s}{S_C}} \tag{25.29}$$

In addition the flux at the sediment-water interface can be determined as

$$J_{out} = S_C L_s \tag{25.30}$$

Because $L_s < H$, the SOD for this case would be less than for Eq. 25.25 because some of the organic carbon is lost as methane bubbles. The gas flux loss can also be quantified as

$$J_{gas} = S_C(H - L_s) \tag{25.31}$$

Finally more useful forms of the flux equations can be developed by substituting Eq. 25.29 into Eqs. 25.30 and 25.31 to yield

$$J_{out} = \sqrt{2Dc_s S_C} \tag{25.32}$$

and

$$J_{gas} = S_C H - \sqrt{2Dc_s S_C} \tag{25.33}$$

Two further modifications can be made by recognizing that the rate of methane production can be related to the incoming carbon flux by

$$S_C = \frac{J_{C\cdot}}{H} \tag{25.34}$$

(where both S_C and $J_{C\cdot}$ are measured in oxygen equivalents), and the diffusion coefficient can be expressed as a mass-transfer coefficient,

$$\kappa_D = \frac{D}{H} \tag{25.35}$$

If we assume that all the methane is completely oxidized in a small aerobic layer at the sediment-water interface, we can then express the maximum carbonaceous SOD as

$$\text{CSOD}_{max} = \sqrt{2\kappa_D c_s J_{C\cdot}} \tag{25.36}$$

EXAMPLE 25.1. MAXIMUM CSOD. Use the model developed above to determine the downward flux of organic carbon that corresponds to the point at which methane becomes saturated for a 10-cm-thick active sediment. Then develop a plot of CSOD_{max} versus downward flux for the same sediment. Note that the diffusion mass-transfer coefficient for methane is 0.00139 m d^{-1}, and $c_s \cong 100$ mgO L^{-1}.

Solution: First, we can combine Eqs. 25.24 [with $c(H) = c_s$], 25.34, and 25.35 and solve for

$$J_{C\cdot} = 2\kappa_D c_s = 2(0.00139)(100) = 0.278 \text{ gO m}^{-2}\text{ d}^{-1}$$

Thus, for carbon fluxes lower than this value, the linear SOD model holds. The square-root relationship of Eq. 25.36 can be used to determine the CSOD for higher values. The results are displayed below.

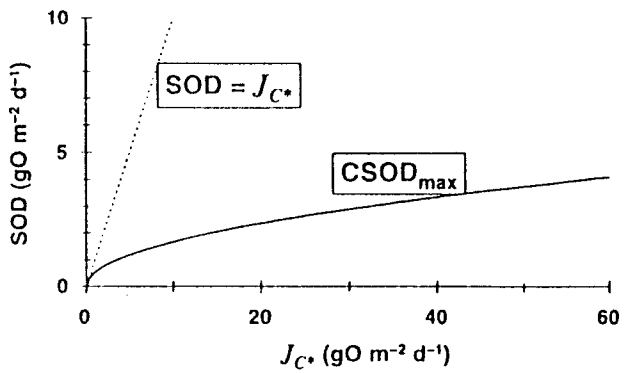

FIGURE E25.1

The foregoing analysis is very important because it provides an explanation for the square-root dependence of SOD on organic carbon. That is, it indicates that the

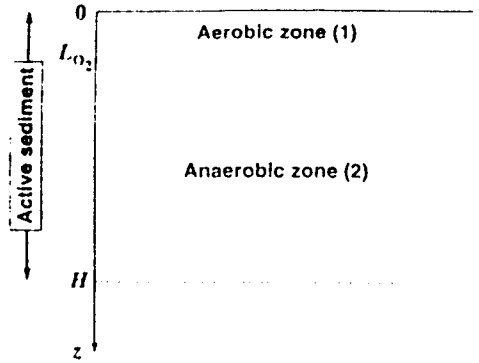

FIGURE 25.8
Segmentation scheme for an active sediment layer composed of aerobic and anaerobic zones.

square-root relationship is caused by carbon losses due to methane bubble formation at high organic carbon levels.

25.4.2 Oxidation in the Aerobic Zone

In the previous section we assumed that all the dissolved methane would be completely oxidized in a thin aerobic layer at the sediment surface. Depending on the relative magnitude of the oxidation reaction and diffusive transport, this might not be true. For example if the oxidation reaction were much slower than the transport, much of the methane would merely pass through the aerobic layer. If such were the case the resulting SOD would be less than computed by Eq. 25.36.

To quantify this effect, methane oxidation can be added to our model. To do this we can write mass balances for each zone in Fig. 25.8.

$$0 = D\frac{d^2c_1}{dz^2} - k_C c_1 \tag{25.37}$$

and

$$0 = D\frac{d^2c_2}{dz^2} + S_C \tag{25.38}$$

where c_1 and c_2 = dissolved methane concentrations in the aerobic and anaerobic zones, respectively, and k_C = decomposition rate of dissolved methane in the aerobic layer. Note that we have omitted the source term (S_C) from Eq. 25.37. Although this assumption is not necessary to obtain a solution, it greatly simplifies the analysis. The omission of the source term can be justified by the fact that, as we will discover, the thickness of the aerobic layer will be much smaller than that of the anaerobic layer. Consequently the methane production in this layer would be dwarfed by the magnitude of the methane flux from the anaerobic zone.

These differential equations are subject to four boundary conditions:

$$c_1(0) = 0 \qquad \text{zero methane at the sediment-water interface} \tag{25.39}$$

$$c_1(L_{O_2}) = c_2(L_{O_2}) \qquad \text{concentration continuity at aerobic-anaerobic interface} \tag{25.40}$$

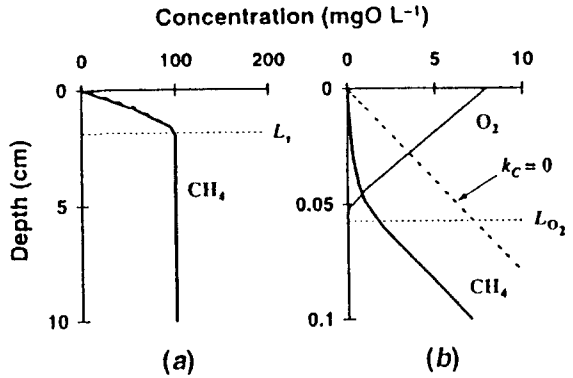

FIGURE 25.9
Profiles of (*a*) methane and (*b*) methane and oxygen for Di Toro's SOD model. The dashed line shows the limiting case where there is no oxidation in the aerobic zone (redrawn from Di Toro et al. 1991).

$$-D\left.\frac{dc_1}{dz}\right|_{z=L_{O2}} = -D\left.\frac{dc_2}{dz}\right|_{z=L_{O2}} \qquad \text{flux continuity at anaerobic-aerobic interface} \tag{25.41}$$

$$c_2(L_s) = c_s \qquad \text{saturation concentration at saturation depth} \tag{25.42}$$

A numerical solution for the active sediment is depicted in Fig. 25.9*a*. This graph shows two cases—with (solid) and without (dashed) oxidation—indicating that the inclusion of oxidation has negligible effect on the profile. However, a blow-up of the aerobic layer in Fig. 25.9*b* shows that oxidation has a major impact within the aerobic layer. Further, the oxygen profile for the aerobic layer, shown in Fig. 25.9*b*, indicates that (1) the aerobic layer is much smaller (on the order of 1 mm) than either the active layer (10 cm) or the undersaturated layer (2 cm), and (2) the oxygen profile is approximately linear.

Although the profiles shown in Fig. 25.9 are instructive, we are presently more interested in the impact of oxidation on the SOD. To quantify this impact, Di Toro et al. (1990) have also developed an analytical solution for the same system. Their solution can be differentiated and substituted into Fick's first law to compute a formula for the flux of dissolved methane at the sediment-water interface,

$$J_{out} = \sqrt{2\kappa_D c_s J_{C^\cdot}}\,\text{sech}(\lambda_C L_{O_2}) \tag{25.43}$$

where

$$\lambda_C = \sqrt{\frac{k_C}{D}} \tag{25.44}$$

and the hyperbolic secant is computed as

$$\text{sech}(x) = \frac{2}{e^x + e^{-x}} \tag{25.45}$$

In addition they computed the flux of methane gas,

$$J_{gas} = J_{C^\cdot} - \sqrt{2\kappa_D c_s J_{C^\cdot}} \tag{25.46}$$

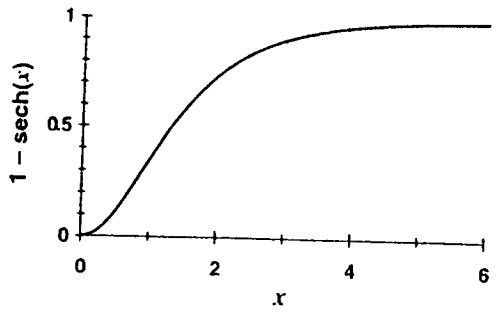

FIGURE 25.10
A plot showing the behavior of 1 − sech(x) versus x.

and the CSOD,

$$\text{CSOD} = \sqrt{2\kappa_D c_s J_{C^\cdot}}[1 - \text{sech}(\lambda_C L_{O_2})] \tag{25.47}$$

Now inspection of Eq. 25.47 indicates that the incorporation of oxidation modifies the former solution (Eq. 25.36) by the term 1 − sech(x). As in Fig. 25.10, this term starts at zero and approaches 1 as x becomes large. In our case Eq. 25.47 will approach Eq. 25.36 when the product of λ_C and L_{O_2} becomes large. The former makes sense because λ_C is directly proportional to k_C and inversely proportional to D. Thus we would expect Eq. 25.47 to approach maximum levels as the oxidation rate increases or the diffusion coefficient decreases. Similarly the latter is reasonable because more oxidation would take place in a larger aerobic zone.

25.4.3 CSOD

The final step in the analysis involves the determination of the thickness of the aerobic layer, L_{O_2}. This can be accomplished by recognizing that the total SOD is the gradient of the pore-water oxygen concentration at the sediment-water interface. Using Fick's first law,

$$\text{SOD} = -D_o \left.\frac{do}{dz}\right|_{z=0} \tag{25.48}$$

where D_o = diffusion coefficient for oxygen in water. The derivative can be approximated by a first-order finite-divided difference (that is, by a straight line),

$$\left.\frac{do}{dz}\right|_{z=0} \cong \frac{o(0) - o(L_{O_2})}{0 - L_{O_2}} = -\frac{o(0)}{L_{O_2}} \tag{25.49}$$

Equation 25.49 can be substituted into Eq. 25.48, which can then be solved for

$$L_{O_2} = D_o \frac{o(0)}{\text{SOD}} \tag{25.50}$$

This result, along with Eq. 25.44, can be used to reformulate the argument of the hyperbolic secant term in Eq. 25.47 as,

$$\lambda_C L_{O_2} = \kappa_C \frac{o(0)}{\text{SOD}} \tag{25.51}$$

where

$$\kappa_C = \sqrt{k_C \frac{D_o^2}{D_c}} \tag{25.52}$$

where we have used the subscript c to distinguish the methane diffusion coefficient (D_c) from that for oxygen (D_o).

Finally Eq. 25.51 can be substituted into Eq. 25.47 to yield the final model of CSOD,

$$\text{CSOD} = \sqrt{2\kappa_D c_s J_{C^\cdot}} \left\{1 - \text{sech}\left[\kappa_C \frac{o(0)}{\text{CSOD}}\right]\right\} \tag{25.53}$$

Note that for low carbon flux ($J_{C^\cdot} < 2\kappa_D c_s$), the square root term is replaced by $J_{C^\cdot}$,

$$\text{CSOD} = J_{C^\cdot} \left\{1 - \text{sech}\left[\kappa_C \frac{o(0)}{\text{CSOD}}\right]\right\} \tag{25.54}$$

Because CSOD is on both sides of these equations, this equation must be solved numerically as a roots problem,

$$f(\text{CSOD}) = J_{C^\cdot} \left\{1 - \text{sech}\left[\kappa_C \frac{o(0)}{\text{CSOD}}\right]\right\} - \text{CSOD} = 0 \tag{25.55}$$

This numerical approach is described in the following example.

EXAMPLE 25.2. CSOD. Develop a plot of CSOD versus downward carbon flux for the same sediment as in Example 25.1. Also, compute the thickness of the aerobic layer for this case. Assume that the oxygen concentration in the overlying water is $o(0)$ = 4 mg L^{-1} and that the reaction coefficient is κ_C = 0.575 m d^{-1}. The diffusion coefficient for oxygen is approximately 2.1 × 10^{-5} cm^2 s^{-1}.

Solution: As an example suppose that the downward flux is 10 gO m^{-2} d^{-1}. This value along with the other model parameters can be substituted into Eq. 25.55 to give

$$f(\text{CSOD}) = 10\left[1 - \text{sech}\left(0.575\frac{4}{\text{CSOD}}\right)\right] - \text{CSOD}$$

The root of this equation can be determined in a number of ways. In this example we use the modified secant method,

$$\text{CSOD} = \text{CSOD} - \frac{\epsilon\text{CSOD} f(\text{CSOD})}{f(\text{CSOD} + \epsilon\text{CSOD}) - f(\text{CSOD})}$$

where ϵ = a small perturbation fraction. An excellent initial guess is provided by Eq. 25.36. For the present case this is

$$\text{CSOD}_{\max} = \sqrt{2(0.00139)100(10)} = 1.6673$$

This value can be substituted into the formula for the modified secant method. If we use a value of ϵ = 0.1, the resulting iterations are

Iteration	CSOD	Approximate error (%)
0	1.6673	
1	1.1557	44.27
2	1.1928	3.1
3	1.1926	0.015

The thickness of the aerobic layer can be calculated as

$$L_{O_2} = 2.1 \times 10^{-5}\ \text{cm}^2\ \text{s}^{-1}\left(\frac{4\ \text{g m}^{-3}}{1.1926\ \text{g m}^{-2}\ \text{d}^{-1}}\frac{\text{m}}{100\ \text{cm}}\frac{10\ \text{mm}}{\text{cm}}\frac{86{,}400\ \text{s}}{\text{d}}\right) = 0.608\ \text{mm}$$

Results for other levels of downward flux are displayed below along with the maximum CSOD values determined previously in Example 25.1. Notice how the inclusion of oxidation reduces the CSOD because some dissolved methane diffuses to the overlying waters before it can be oxidized.

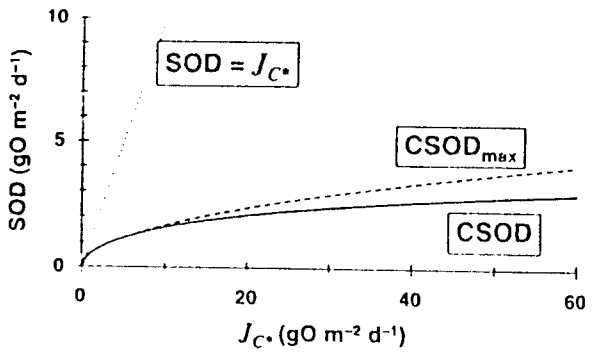

FIGURE E25.2

25.4.4 Nitrogen and Total SOD

Using a similar analysis as applied to carbon, Di Toro et al. (1990) also evaluated the effect of nitrification on SOD. As depicted in Fig. 25.5*b* nitrogen differs from carbon in that the ammonium formed from organic nitrogen does not become saturated and form bubbles as was the case for the methane from organic carbon.

This difference is accounted for by the following equation for the total SOD due to both carbon and nitrogen,

$$\text{SOD} = \underbrace{\sqrt{2\kappa_{DC_s}J_{C*}}\left\{1 - \text{sech}\left[\kappa_C\frac{o(0)}{\text{SOD}}\right]\right\}}_{\text{CSOD}} + \underbrace{r'_{on}a_{no}J_{C*}\left\{1 - \text{sech}\left[\kappa_N\frac{o(0)}{\text{SOD}}\right]\right\}}_{\text{NSOD}} \tag{25.56}$$

where

$$\kappa_N = \sqrt{k_N\frac{D_o^2}{D_n}} \tag{25.57}$$

where k_N = oxidation rate of ammonium to nitrogen gas and D_n = diffusion coefficient for ammonium ion in water. Note that again for low carbon flux ($J_{C*} < 2\kappa_{DC_s}$), the square-root term is replaced by J_{C*},

$$\text{SOD} = J_{C*}\left\{1 - \text{sech}\left[\kappa_C\frac{o(0)}{\text{SOD}}\right]\right\} + r'_{on}a_{no}J_{C*}\left\{1 - \text{sech}\left[\kappa_N\frac{o(0)}{\text{SOD}}\right]\right\} \tag{25.58}$$

Inspection of Eq. 25.56 shows that the NSOD is mathematically similar to the CSOD. The differences relate to the conversion of the carbon flux into nitrogenous oxygen demand ($r'_{on}a_{no}$) and the absence of the square-root term because of the lack of gas formation in the anaerobic layer. However, as with CSOD, the hyperbolic secant term accounts for both the diffusion/reaction competition in the aerobic zone and the shutdown of SOD at low oxygen levels. As was the case for Eqs. 25.53 and 25.54, because SOD appears on both sides of Eqs. 25.56 and 25.58, they must be solved numerically as a roots problem.

EXAMPLE 25.3. TOTAL SOD. Develop a plot of total SOD versus downward carbon flux for the same sediment as was studied in Examples 25.1 and 25.2. Assume that the parameters have the following values: $\kappa_N = 0.897\ \text{m d}^{-1}$, $r'_{on} = 1.714\ \text{gO gN}^{-1}$, and $a_{no} = 0.0654\ \text{gN gO}^{-1}$.

Solution: As with Example 25.2, suppose that the downward flux is 10 gO m^{-2} d^{-1}. This value along with the other model parameters can be substituted into Eq. 25.56 to give

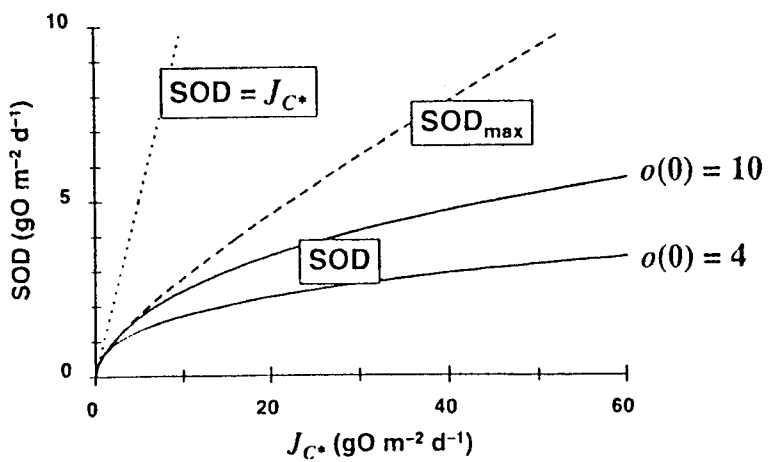

FIGURE E25.3

$$f(\text{SOD}) = \sqrt{2(0.00139)100(10)}\left[1 - \text{sech}\left(0.575\frac{4}{\text{SOD}}\right)\right] + 1.714(0.0654)(10)\left[1 - \text{sech}\left(0.897\frac{4}{\text{SOD}}\right)\right] - \text{SOD}$$

The root of this equation can be determined with the modified secant method, with an initial guess provided by

$$\text{CSOD}_{\max} = \sqrt{2\kappa_D c_s J_C} + r'_{on} a_{no} J_C$$

This value can be substituted into the formula for the modified secant method. The results along with SODs for other flux rates are displayed in Fig. E25.3. In addition the plot shows results when the oxygen in the water is raised to 10 mg L^{-1}. As expected this leads to higher SODs.

Before proceeding, let's regroup and consider what the analytical model tells us about SOD:

1. If there is oxygen in the overlying water, oxidation of methane and ammonium takes place in a very thin aerobic layer at the sediment-water interface.
2. In the thin aerobic layer a competition exists between the oxidation reaction and diffusion. The 1 − sech terms in Eq. 25.58 account for this competition as well as the suppression of SOD when oxygen in the overlying water gets low.
3. Methane can exceed its saturation concentration in the anaerobic sediments. Consequently bubbles can be lost from the system, as reflected by the square-root term in Eq. 25.58. Because ammonium does not form a gaseous phase at the pHs encountered in sediments, the relationship of NSOD to downward oxygen-equivalent flux in Eq. 25.58 is linear.

By providing a means to calculate SOD as a function of external loadings, the Di Toro framework is a major advance over prior schemes. Predictions should be more realistic than those obtained with the two alternatives used by earlier modelers: fixed SOD or a linear decrease in proportion to load reductions. The former is overly conservative whereas the latter is overly optimistic. By allowing a more physically realistic middle course, the Di Toro approach should provide a basis for better management decisions. Most importantly it allows SOD to be computed internally in a mechanistic fashion rather than in a prescribed or empirical manner. To date Di Toro's framework has been applied to the Chesapeake Bay (Cerco and Cole 1993, Di Toro and Fitzpatrick 1993). In the coming years numerical versions of the approach will undoubtedly be incorporated into most water-quality models to provide a more rigorous characterization of SOD.

25.5 NUMERICAL SOD MODEL

Although the analytical solution is elegant and instructive, numerical solution techniques provide greater flexibility and broader application. The following models are similar in spirit to the approach outlined by Di Toro and Fitzpatrick (1993)

for estuarine systems. However, in this section we limit our discussion to the freshwater case. At the end of the discussion we will describe how estuarine systems differ from freshwater environments.

In this section we first describe a simplified SOD model that focuses on ammonium creation and oxidation. Later we will incorporate carbon and other elements into the framework.

As in Fig. 25.11, we can represent the active sediments as two well-mixed layers. Notice that in contrast to the analytical model, we are representing the downward flux of organic matter in carbon units (rather than oxygen equivalents).

A mass balance can be written for organic carbon in the lower sediment layer as

$$V_2\frac{dc_2}{dt} = J_C A_s - k_{c2} V_2 c_2 \tag{25.59}$$

where c_2 = concentration of organic carbon (gC m^{-3})
J_C = flux of organic carbon settling from the overlying water (gC m^{-2} d^{-1})
A_s = surface area of the sediment-water interface (m^2)
k_{c2} = first-order diagenesis rate of organic carbon (d^{-1})

Now because the surface area between all the model segments is equal to A_s and $V_2 = A_s H_2$, we can divide both sides of the balance by A_s to yield

$$H_2\frac{dc_2}{dt} = J_C - k_{c2} H_2 c_2 \tag{25.60}$$

Thus we have expressed the mass balance in terms of flux (M L^{-2} T^{-1}) rather than rate of mass transfer (M T^{-1}). Similar flux balances can be written for ammonium as

$$H_2\frac{dn_2}{dt} = a_{nc} k_{c2} H_2 c_2 + v_{dn12}(n_1 - n_2) \tag{25.61}$$

and

$$H_1\frac{dn_1}{dt} = v_{dn12}(n_2 - n_1) - v_{dnw1} n_1 - k_{n1} H_1 n_1 \tag{25.62}$$

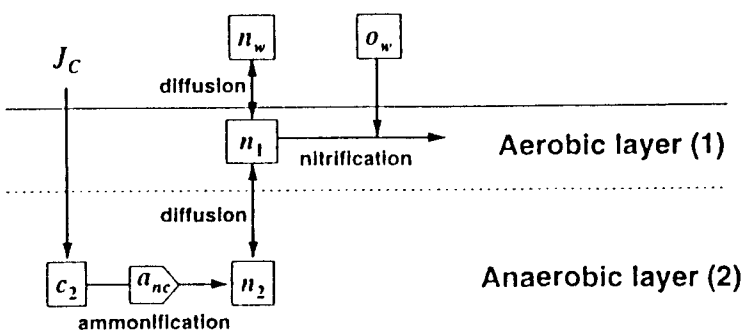

FIGURE 25.11
Schematic of a control-volume approach for modeling NSOD.

where n = ammonium concentration expressed as nitrogen (gN m^{-3})
v_{dn12} = diffusive mass-transfer coefficient between the two layers (m d^{-1})
v_{dnw1} = diffusive mass-transfer coefficient between the surface layer and the water (m d^{-1})
k_{n1} = nitrification rate of ammonium in the surface layer (d^{-1})

Notice that Eq. 25.62 assumes that the ammonium concentration of the overlying water is negligible. Although this will not necessarily be true, we have adopted this assumption to be consistent with the analytical framework. Also recognize that the mass-transfer coefficients can be related to more fundamental parameters by

$$v_{dn12} = \frac{D_n}{H_{12}} \qquad v_{dnw1} = \frac{D_n}{H_{w1}} \tag{25.63}$$

where D_n = diffusion coefficient for ammonium in water (m^2 d^{-1}) and H_{12} and H_{w1} = mixing lengths for the two diffusive transfer processes (m).

As described later these balances can be solved numerically to simulate the concentrations as a function of time. Before doing this it is instructive to first solve them at steady-state. Along with insight into how the model functions, such solutions allow direct comparison between our lumped, numerical characterization and Di Toro's distributed, analytical solution.

After setting Eqs. 25.60 to 25.62 to steady-state, Eq. 25.60 can be solved for

$$c_2 = \frac{J_C}{k_{c2}H_2} \tag{25.64}$$

which in turn can be substituted into Eq. 25.61,

$$0 = a_{nc}J_C + v_{dn12}(n_1 - n_2) \tag{25.65}$$

Next Eqs. 25.65 and 25.62 can be added to eliminate n_2,

$$0 = a_{nc}J_C - k_{n1}H_1n_1 - v_{dnw1}n_1 \tag{25.66}$$

This equation can then be solved for

$$n_1 = \frac{a_{nc}J_C}{k_{n1}H_1 + v_{dnw1}} \tag{25.67}$$

which can then be substituted back into Eq. 25.62 to give,

$$n_2 = \frac{v_{dn12} + k_{n1}H_1 + v_{dnw1}}{v_{dn12}(k_{n1}H_1 + v_{dnw1})}a_{nc}J_C \tag{25.68}$$

Therefore Eqs. 25.64, 25.67, and 25.68 provide steady-state solutions for all the variables as a function of the organic carbon flux.

Oxygen demand can be integrated into the framework by recognizing that the oxygen concentration profile through the surface layer is very close to being linear. Thus the SOD at the sediment-water interface can be nicely approximated by the following simple expression of Fick's first law (recall Eq. 25.50),

$$\text{SOD} = \frac{D_o}{H_1}o_w \tag{25.69}$$

where D_o = oxygen diffusion coefficient (m^2 d^{-1}). Now it can be recognized that the SOD is also equivalent to the rate at which ammonium is being oxidized,

$$\text{SOD} = r'_{on}k_{n1}H_1n_1 \tag{25.70}$$

where r'_{on} = oxygen demand for nitrification/denitrification (according to Eq. 25.18, 1.714 gO gN^{-1}). Assuming that $H_{w1} = H_1$, Eqs. 25.67 and 25.69 can be substituted into Eq. 25.70 and the result manipulated to give

$$\text{NSOD} = r'_{on}a_{nc}J_C\frac{1}{1 + \dfrac{D_n\text{NSOD}^2}{D_o^2o_w^2k_{n1}}} \tag{25.71}$$

where we have changed SOD to NSOD to acknowledge that we are presently limiting ourselves to ammonium oxidation. This equation can be solved numerically for NSOD. This result can then be used in conjunction with Eq. 25.69 to solve for the thickness of the aerobic layer.

Thus Eq. 25.71 is a simple finite-difference representation of the analytical approach which for NSOD is the second part of Eq. 25.56,

$$\text{NSOD} = r'_{on}a_{nc}J_C\left[1 - \text{sech}\left(\sqrt{k_{n1}\frac{D_o^2}{D_n}}\frac{o_w}{\text{NSOD}}\right)\right] \tag{25.72}$$

EXAMPLE 25.4. COMPARISON OF LUMPED AND DISTRIBUTED NSOD. Develop a plot of NSOD versus downward carbon flux for the same sediment as was studied in Examples 25.1 through 25.3 using both the distributed and lumped NSOD models. Assume that the parameters have the following values: o_w = 10 mg L^{-1}, κ_N = 0.897 m d^{-1}, r'_{on} = 1.714 gO gN^{-1}, $D_o = 1.73 \times 10^{-4}$ m^2 d^{-1}, $D_n = 8.47 \times 10^{-5}$ m^2 d^{-1}, and a_{nc} = 0.176 gN gC^{-1}.

Solution: First, we must determine the nitrification rate from Eq. 25.57,

$$k_{n1} = \kappa_N^2\frac{D_n}{D_o^2} = 0.897^2\frac{8.47 \times 10^{-5}}{(1.73 \times 10^{-4})^2} = 2282 \text{ d}^{-1}$$

Next the parameter values can be substituted into Eq. 25.72 to obtain the distributed solution. For example for the case where J_{C^*} = 10 gO m^{-2} d^{-1} (which corresponds to J_C = 3.75 gC m^{-2} d^{-1}),

$$\text{NSOD} = 1.714(0.176)3.75\left\{1 - \text{sech}\left[\sqrt{2282\frac{(1.73 \times 10^{-4})^2}{8.47 \times 10^{-5}}}\frac{10}{\text{NSOD}}\right]\right\}$$

which can be solved iteratively for NSOD = 1.130 gO m^{-2} d^{-1}.

In a similar fashion the lumped case can be set up for Eq. 25.71,

$$\text{NSOD} = 1.714(0.176)3.75\frac{1}{1 + \dfrac{8.47 \times 10^{-5}\text{NSOD}^2}{(1.73 \times 10^{-4})^2(10)^2 2282}}$$

which can be solved for 1.113 gO m^{-2} d^{-1}. Thus the approaches yield similar results. Additional solutions are displayed in the plot shown in Figure E25.4:

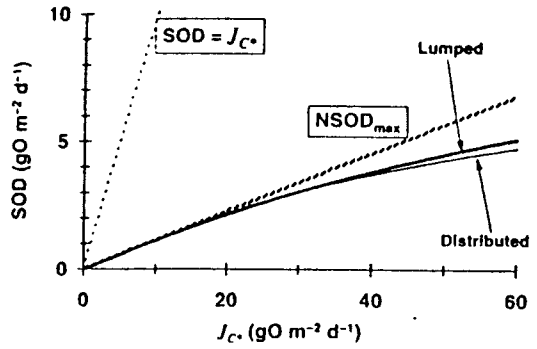

FIGURE E25.4

25.6 OTHER SOD MODELING ISSUES (ADVANCED TOPIC)

At the time of this book's publication, SOD modeling is an active and rapidly evolving research area. Consequently there are a number of relevant issues that are currently unresolved and that were not included in the prior sections. Because these topics are highly relevant to how SOD will be computed in the coming years, they are the focus of this section.

25.6.1 Methane Bubble Formation

Although the foregoing section shows how numerical, finite-difference methods can be developed, it did not address the issue of methane bubble formation in the anaerobic sediments. The simplest approach is merely to model methane in a fashion similar to ammonium, as in

$$H_2\frac{dc_2}{dt} = J_C - k_{c2}H_2c_2 \tag{25.73}$$

$$H_2\frac{dm_2}{dt} = k_{c2}H_2c_2 + v_{dm12}(m_1 - m_2) \tag{25.74}$$

$$H_1\frac{dm_1}{dt} = v_{dm12}(m_2 - m_1) - v_{dmw1}m_1 - k_{m1}H_1m_1 \tag{25.75}$$

Once the deep aerobic layer methane exceeds saturation, it can be kept fixed at the saturation level. This means that Eq. 25.75 becomes

$$H_1\frac{dm_1}{dt} = v_{dm12}(c_s - m_1) - v_{dmw1}m_1 - k_{m1}H_1m_1 \tag{25.76}$$

At this point this equation can be directly solved for the methane concentration and SOD in a fashion similar to the derivation of Eq. 25.71.

Although this approach may seem appealing, it has one major flaw. That is, once the saturation is exceeded, the CSOD becomes constant. Thus the square root

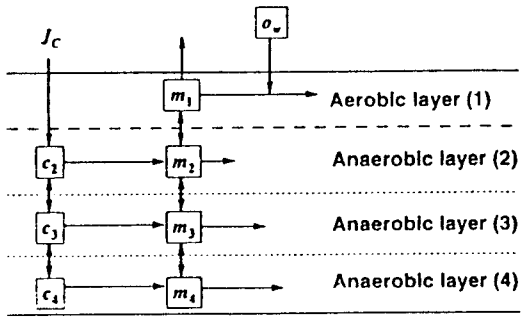

FIGURE 25.12
Schematic of a control-volume approach for modeling CSOD in freshwater systems with methane formation.

relationship manifested by the analytical solution does not occur. This problem is compounded because the saturation is usually exceeded at low organic carbon flux. Thus not only does the CSOD hit a ceiling, but it does so at an unrealistically low level.

A remedy for this problem is depicted in Fig. 25.12. By dividing the anaerobic zone into layers, the saturation phenomena will come into play in stages rather than at a single instant. In other words, the lowest layer will saturate first at which point its level becomes fixed. Thereafter, the middle and then the top layer will saturate. Once all layers saturate, the CSOD will be fixed. However, the sequential saturation up to that point will follow the analytical solution nicely. In addition it extends the validity of the approximation to higher levels than would be the case for the single layer.

25.6.2 Time-Variable SOD Calculations

To this point we have focused on steady-state computations. For most water-quality problems, time-variable solutions would be of equal, if not greater, importance. The most straightforward approach would be to merely integrate the equations numerically using either explicit or implicit numerical algorithms as described previously in Lecs. 7 and 11 through 13. For example Eqs. 25.60 to 25.62 could be integrated to determine time-variable NSOD.

Although this is a viable option, a problem arises in that the thin surface layer requires much finer temporal resolution (that is, a much smaller time step) to attain stable solutions than does the thicker anaerobic layer. In numerical methods this is referred to as a "stiff" solution.

This apparent dilemma leads to a beneficial insight. As recognized by Di Toro and Fitzpatrick (1993), because it is much thinner, the surface layer will always be at a steady-state relative to the time frame needed to resolve variations in the thicker anaerobic layer.

Consequently Eq. 25.62 can be solved at steady-state for

$$n_1 = R_{12}n_2 = \frac{v_{dn12}}{v_{dn12} + v_{dnw1} + k_{n1}H_1}n_2 \tag{25.77}$$

where R_{12} = ratio of the ammonium concentration in the aerobic (1) to the anaerobic layer (2). This value can then be substituted into Eq. 25.61 to give

$$H_2\frac{dn_2}{dt} = a_{nc}k_{c2}H_2c_2 + v_{dn12}(R_{12} - 1)n_2 \tag{25.78}$$

Thus instead of integrating three differential equations (one of which is less stable than the other two), we integrate the two more robust ODEs (Eqs. 25.60 and 25.78) and determine the third unknown, n_1, algebraically with Eq. 25.77. Note that this trick applies equally well to methane and CSOD as well as to other elements involved in sediment calculations.

25.6.3 Water Boundary Layer

In Example 25.4 a very high nitrification rate is needed so that the model as originally formulated yields realistic NSOD values. A similar conclusion can be also made for CSOD. In general, biologically mediated reactions such as nitrification and methane oxidation generally proceed at rates on the order of 0.01 to 5 d^{-1} rather that the magnitude of 1000 to 10,000 d^{-1} used in Example 25.4.

One reason for the high rates is that sediments have much higher bacterial biomass than the water. A second explanation lies in Di Toro's assumption that all the decomposition takes place in a thin aerobic sediment layer. Although this assumption was certainly valid from Di Toro's perspective and does not negate his conclusion, it must now be reexamined as we begin to integrate the mechanistic SOD model into large water-quality-modeling frameworks.

As depicted in Fig. 25.13, along with the sediment layers, a laminar boundary layer can exist in the water. The size of the two layers would be determined by different processes. The aerobic sediment layer thickness would be dictated by the balance between oxygen consumption and diffusion as expressed by Eqs. 25.69 and 25.70. In contrast the water boundary layer is an artifact of the turbulence in

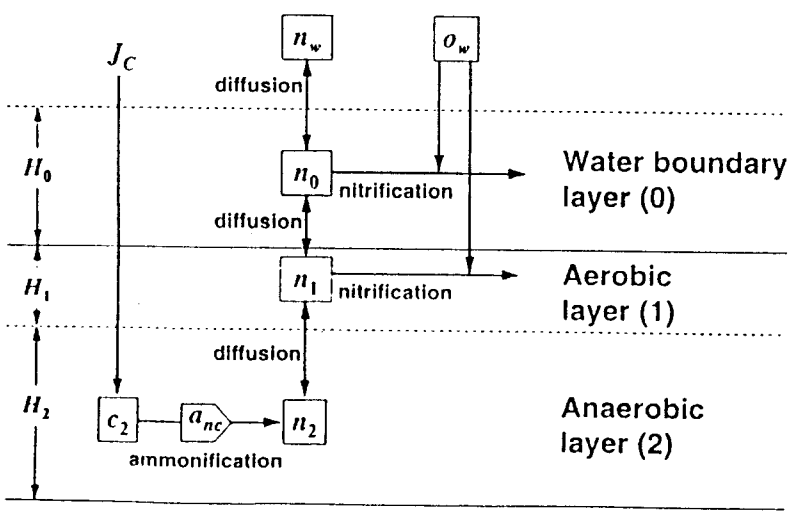

FIGURE 25.13
An NSOD model including a water laminar boundary layer.

the water. Thus for deeper waters with relatively low flows (for example, deeper lakes and estuaries), such a boundary layer can be significant. Consequently it could serve as a compartment where additional oxidation could take place.

The foregoing finite-difference models can be extended to account for such a layer. For example mass balances can be written for ammonium as

$$H_2\frac{dn_2}{dt} = a_{nc}k_{c2}H_2c_2 + v_{dn12}(n_1 - n_2) \tag{25.79}$$

$$H_1\frac{dn_1}{dt} = v_{dn12}(n_2 - n_1) + v_{dn01}(n_0 - n_1) - k_{n1}H_1n_1 \tag{25.80}$$

$$H_0\frac{dn_0}{dt} = v_{dn01}(n_1 - n_0) + v_{dnw0}(n_w - n_0) - k_{n0}H_0n_0 \tag{25.81}$$

Notice how we have now included the ammonium concentration in the overlying water, n_w.

At steady-state these equations can be solved simultaneously (along with Eq. 25.60) for the organic carbon and the ammonium concentrations. The values of ammonium for the upper two layers can then be substituted into the following relationship for SOD:

$$\text{SOD} = r'_{on}(k_{n1}H_1n_1 + k_{n0}H_0n_0) \tag{25.82}$$

This formula can be combined with Eq. 25.69 in order to develop an iterative method for determining the SOD.

Although the foregoing analysis provides an indication of the importance of the water boundary layer, it suffers in that the thickness of the boundary layer must be given. A superior approach would link the transfer in this layer to the flow velocity in the overlying water. Recent efforts are being made to develop such relationships (Nakamura and Stefan 1994).

25.6.4 Nitrate and Phosphate

Because of our present emphasis on oxygen, all the other compounds discussed to this point (ammonium, methane) directly impact SOD. However, beyond these compounds there are a variety of others that are important and are significantly affected by oxygen.

Nitrate. Nitrate is an important plant nutrient that is released during nitrification. To this point we have assumed that it is totally reduced to nitrogen gas by denitrification. Although this is a reasonable first assumption that works well for many systems, a more refined viewpoint would consider that only part of the generated nitrate flux would be denitrified and part released to the overlying water. Di Toro and Fitzpatrick (1993) show how this can be done by slightly modifying the SOD model described previously.

First, nitrate is modeled explicitly. For the two-layer model, balances would be written as

$$H_2\frac{di_2}{dt} = v_{dn12}(i_1 - i_2) - k_{i2}H_2i_2 \tag{25.83}$$

and

$$H_1\frac{di_1}{dt} = v_{dn12}(i_2 - i_1) - v_{dnw1}(i_0 - i_1) + k_{n1}H_1n_1 - k_{i1}H_1i_1 \tag{25.84}$$

where i = nitrate concentration (mgN L^{-1}) and k_i = denitrification rate (d^{-1}). For the steady-state case these equations can be solved for i_1 and i_2. These values, in turn, can be used to compute the flux of nitrogen gas that would be created and lost from the sediments,

$$J_N = k_{i1}H_1i_1 + k_{i2}H_2i_2 \tag{25.85}$$

This value is then used to correct the carbon flux to acknowledge that methane is utilized during denitrification. The final model for conditions below methane saturation would look like

$$\text{SOD} = r_{oc}(J_C - a_{cn}J_N)\frac{1}{1 + \dfrac{D_c\text{SOD}^2}{D_o^2o_w^2k_{m1}}} + r_{on}a_{nc}J_C\frac{1}{1 + \dfrac{D_n\text{SOD}^2}{D_o^2o_w^2k_{n1}}} \tag{25.86}$$

where a_{cn} = methane loss due to denitrification = 1.07 gC gN^{-1}. Also, since we are directly discounting the CSOD, the true nitrification oxygen demand r_{on} = 4.57 gO gN^{-1} is used for the NSOD.

Phosphate. Phosphorus is another important plant nutrient that is greatly affected by sediment oxygen levels. However, in contrast to nitrate its accurate modeling involves some major modifications. In particular the dynamics of phosphorus are significantly dictated by its association with particulate matter in the sediments.

A number of investigators starting with Mortimer (1941, 1942) have theorized that phosphorus in the aerobic surface layer is sorbed to precipitated iron hydroxides. Such attachment then impedes its transfer back into the water. When oxygen levels drop, the iron hydroxides are dissolved as they become reduced. This leads to an associated release of dissolved phosphorus into the sediment pore waters where it is free to diffuse into the overlying water.

These effects can be integrated into the SOD framework by writing balances for phosphate that account for the sorption mechanism,

$$H_2\frac{dp_2}{dt} = a_{pc}k_{c2}H_2c_2 + v_{dp12}(F_{d1}p_1 - F_{d2}p_2) + v_{dp12}(F_{p1}p_1 - F_{p2}p_2) + v_h(p_1 - p_2) \tag{25.87}$$

$$H_1\frac{dp_1}{dt} = v_{dp12}(F_{d2}p_2 - F_{d1}p_1) + v_{dp12}(F_{p2}p_2 - F_{p2}p_1) + v_{dmw1}(F_{dw}p_2 - F_{d1}p_1) \tag{25.88}$$

where F_d and F_p are the fractions associated with dissolved and particulate forms in the two layers. Later in this book when we discuss toxic substances, we will describe how they are derived. For the time being they can be calculated by

$$F_d = \frac{1}{\phi + K_{dp}(1 - \phi)\rho} \qquad F_p = \frac{K_{dp}(1 - \phi)\rho}{\phi + K_{dp}(1 - \phi)\rho} \tag{25.89}$$

where ϕ = sediment porosity ($\cong$ 0.8 to 0.95)
ρ = sediment density ($\cong 2.5 \times 10^6$ g m^{-3})
K_{dp} = phosphorus sorption coefficient (m^3 g^{-1})

The sorption coefficient is the key to the phosphorus model. At high values ($\cong$ 0.01 to 0.001 m^3 g^{-1}), the dissolved concentration will be low and diffusion in the pore water will be low. Conversely at low values of K_{dp} ($\cong$ 0.00005 to 0.0005 m^3 g^{-1}), pore water concentration and diffusion become high.

Aside from sorption, three additional features of Eqs. 25.87 and 25.88 bear mention. First, notice that I have included terms for particle mixing. Such transport is due to burrowing and other activities of benthic organisms. Second, I have included an advective term to account for the movement of matter away from the sediment-water interface due to the accumulation of settling solids in the sediments. Finally I should mention that whereas we have used the steady-state case for all previous constituents, it is not meaningful for a substance like phosphorus that is not continuously subject to a constant diffusion mechanism. Thus, unless the overlying water is always aerobic (in which case the phosphorus flux would probably be negligible anyway), phosphorus in the anaerobic layer must be simulated dynamically.

25.6.5 Estuaries

Because of the dominant role of sulfur, estuaries tend to exhibit a different carbon chemistry from freshwater systems like lakes and streams. In essence the SOD is tied to the reduction of sulfate (SO_4) to produce sulfide (H_2S). The key reaction is (Barnes and Goldberg 1976)

$$2CH_2O + H_2SO_4 \rightarrow 2CO_2 + H_2S + 2H_2O \tag{25.90}$$

In the anaerobic zone, sulfide is produced. A portion of it reacts with iron to form particulate iron sulfide [FeS(*s*)]. The remainder diffuses into the aerobic zone where a part is oxidized. In addition particle mixing can move some of the particulate iron sulfide into the aerobic zone where it can be oxidized to form ferric oxyhydroxide [$Fe_2O_3(s)$], again consuming oxygen in the process.

Thus the model would be quite similar in format to the balances for phosphorus, with the exception that

- Sulfide is modeled in place of phosphorus.
- Sulfide undergoes oxidation in the surface layer.
- Precipitation reactions would not depend on oxygen in the way that phosphate sorption does.

Di Toro and Fitzpatrick (1993) provide a very thorough description of this sulfide model along with all the other elements of SOD modeling discussed in this lecture.

Finally, it should be noted that sulfur plays an important role in many freshwater sediments. In the future, sulfur dynamics must be incorporated into SOD frameworks developed for such systems.

PROBLEMS

25.1. A small pond located at 10,000 ft has the following characteristics:

Residence time = 1 wk
Area = 1×10^5 m^2
Mean depth = 2 m

The pond has an inflow CBOD concentration of 50 mg L^{-1}. The CBOD does not settle but decays at a rate of 0.05 d^{-1} at 20°C. The temperature of the pond is 15°C. The wind speed over the pond is 2 m s^{-1}. The inflow has a temperature of 10°C and a deficit of 3 mg L^{-1}. Half of the sediments exert no SOD whereas the other half exert an SOD of 0.2 g m^{-2} d^{-1} at 20°C. Compute the following (don't forget temperature correction factors):

(*a*) The CBOD concentration of the system
(*b*) The oxygen saturation concentration for the pond (use of table in App. B is acceptable)
(*c*) The reaeration rate for the pond at 15°C (units of d^{-1})
(*d*) The oxygen concentration of the pond

25.2. The epilimnion of a lake has a particulate organic carbon concentration of 1 mg L^{-1} and a dissolved oxygen concentration of 9 mg L^{-1}. The carbon settles at a rate of 0.05 m d^{-1} and is oxidized in the hypolimnion at a rate of 0.05 d^{-1}. The bulk diffusion coefficient across the thermocline is 0.05 m d^{-1} and the hypolimnion thickness is 5 m. The situation is depicted in the following diagram:

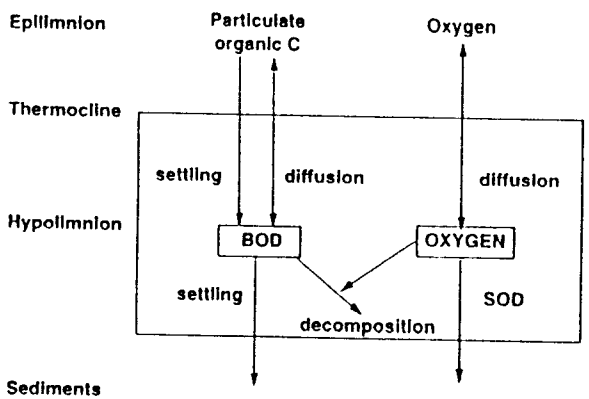

FIGURE P25.2

(*a*) Compute the steady-state concentration of carbonaceous BOD and dissolved oxygen in the hypolimnion. Assume that the epilimnion levels are constant and that once the particulate matter settles to the bottom it does not exert an SOD.
(*b*) For the case described in (*a*) compute the SOD that would be exerted by the particulate matter that settles from the hypolimnion to the sediments using the naive Streeter-Phelps SOD model described in Sec. 25.2. Assume that the particulate matter is completely oxidized in the sediments. Express the resulting SOD in units of g m^{-2} d^{-1}.

25.3. Repeat Example 25.2, but for a downward flux of 20 gO m^{-2} d^{-1} and a water oxygen concentration of 3 mg L^{-1}.

25.4. A lake has a particulate organic carbon concentration of 5 mg L^{-1} that settles at a rate of 0.25 m d^{-1}. Determine the steady-state SOD and the thickness of the aerobic layer for the system if the overlying water has an oxygen concentration of 4 mg L^{-1}. The active sediment layer is 10 cm thick and assume that all the nitrate produced by nitrification is denitrified to nitrogen gas. Assume that there is no water boundary layer.
(*a*) Use the analytical solution to obtain your answer.
(*b*) Use a numerical approach with the anaerobic sediments divided into four segments.

25.5. Repeat Prob. 25.4, but add a 1-cm-thick boundary layer in the water. Assume that diffusion and reaction in both the sediment aerobic and water boundary layers are the same.